ReaxFF Simulation of Pyrolysis Behaviors of Polysiloxane Precursors with Different Carbon Content

Journal:	*Chemistry of Materials*
Manuscript ID	cm-2023-00010y.R2
Manuscript Type:	Article
Date Submitted by the Author:	n/a
Complete List of Authors:	Chaney, Harrison; Virginia Tech Lu, Kathy ; Virginia Polytechnic Institute and State University, Materials Science & Engineering

ReaxFF Simulation of Pyrolysis Behaviors of Polysiloxane Precursors with Different Carbon Content

Harrison Chaney, Kathy Lu*

Department of Materials Science and Engineering, Virginia Polytechnic Institute and State University, Blacksburg, Virginia, 24061, USA

*Corresponding author: Email: klu@vt.edu

Abstract: Polymer derived ceramics are a promising class of high temperature materials. This work uses LAMMPS and a Reactive Force Field (ReaxFF) energy potential to first time quantify the atomic evolution of the polymer to ceramic conversion. Three different polymer structures are selected based on initial carbon content and molecular structure differences. From these simulations, ceramic composition, yield, atomic structure, bond change, and radial distribution function (RDF) are comprehensively analyzed and provided data that are not available otherwise. The ceramic compositions correlate with the polymer compositions. The C-rich precursor forms C-C bonds through Si-O, Si-C, and C-H bond losses while less C-rich polymers have no significant C-C bond formation during C-H bond loss. The end structures have vastly different Si-O rich and C-rich domain sizes, which cannot be observed by any bulk analysis. For the first time, H presence and cluster separation are shown to be determined by the polymer molecular structure. The RDF results show that higher pyrolysis temperature leads to more C-C bond formation. Even at 2100 K, C-H bonds are still prevalent and there is no long-range ordering. Such fundamental understanding provides new knowledge about polymer atomic evolution to silicon oxycarbide (SiOC) ceramics.

1. Introduction

Polymer derived ceramics are highly tunable species created through pyrolysis of Si-containing polymers.[1, 2] SiOC materials made with this method are of particular interest because of their unique ability to obtain near net shapes at lower temperatures than in traditional ceramics.[3] The applications of SiOC systems include coatings,[4] microwave absorbing devices,[5] and high temperature components.[6] Among these, the most studied system is SiOC-based systems.[4, 6] The starting materials include a Si-O backbone with -H, $-CH_3$, $-C_2H_3$, and $-C_6H_5$ side groups; the pyrolyzed phases include an amorphous SiOC and different C regions.

The polymer to ceramic conversion is a drastic process involving cleavage of Si-H and Si-C bonds, dehydrogenation of phenyl rings and $-CH_3$ groups, radical species generation, and new phase formation. Different phases developed in the system are highly dependent upon pyrolysis temperature and precursor(s).[4, 5, 7, 8, 9] A number of ring species can also form from the polymer decomposition, including cyclic SiO species with some of the side groups still remaining intact.[8, 9] Si-Si bonding may occur in these cyclic intermediates.[10] Many of the C side groups have been observed in the off-gas. An increase in Si-C bond breakage is observed from 600 to 1100°C.[11] At ~1250°C, glassy carbon and SiOC phase(s) can be observed.[12] At pyrolysis temperatures of 1300°C and higher, amorphous SiO_x and SiC become observable along with the existing amorphous C phase.[12] Regions of SiC and graphitic C become more prevalent as the temperature is further increased to > 1300°C.[2, 10]

The composition of the final ceramics can be adjusted through initial composition, choice of the dispersion solvent for polymer precursors (if used), and pyrolysis conditions.[2, 13-15] Different combinations of C-containing side groups on the polysiloxane backbone yield different structures.

Higher pyrolysis temperatures result in higher levels of carbon.[2] Narrowing of diffraction peaks and increasing peak intensity are associated with higher pyrolysis temperatures.[16]

While the general process of polymer conversion to ceramics has been described based on experimental studies,[15,17] many aspects remain to be understood with the decomposition of the polymer precursors, e.g., how the initial polymer composition impacts the end composition and atomic structure as well as how different pyrolysis temperatures affect the formation of the ceramic species. There is also a lack of experimental means to describe atomic structural evolution, quantify different bonds, and obtain the corresponding atomic RDF, e.g., how SiOC, SiO_2, SiC, and C form and evolve. Other aspects to understand include the specific effects that carbon side groups have on bond breakage and formation of Si-O, C-C, and even Si-Si intermediate bonds.

Simulations can be used to show chain break-up and re-formation, fugitive species escape, and regions of SiOC and amorphous C that cannot be distinguished with experimental methods. Simulations can also show the RDF and end compositions of SiOC ceramics.[18, 19] There have been several efforts simulating the amorphous phases of polymer derived ceramics using ReaxFF.[18-22] Chenworth simulated the pyrolysis of polydimethylsiloxane (PDMS) in the presence of water, NO, and ozone at 2500 K.[23] Naserifar et al.[24] heated a hydridopolycarbosilane (HPCS) polymer structure to 5000 K and simulated the polymer decomposition. It was found that the C-H and Si-H bonds began to break at ~1000 K while the Si-C cleavage was not initiated until 2000 K and was further quickened when the temperature was increased to 2400 K.

A blend of HCPS and polyhydromethylsiloxane (PHMS) was heated to 1800 K and maintained for 4.7 ns until all H atoms were eliminated.[10] Si-H, C-H, and Si-CH_3 bonds were broken at 1000 K while C-C bond formation increased at 1800 K. In addition, a new force field parameter was applied to the simulations of PHMS/HCPS.[25] The polymer precursor blend was

first allowed to stabilize and then progressively heated. When the temperature increased to 2500 K, which met the before-mentioned threshold of accelerated Si-C bond breakage, the simulation was able to illustrate phase separation and achieve experimentally verifiable end compositions.[25] In both studies,[10, 25] a script was used to delete the gas species in a fixed interval of time. In a different study, the molecular weight threshold for the gas deletion included single and double carbon species[26] in 10 ps and 5 ps intervals respectively. However, the system used less than 10,000 atoms, which was too small to realistically illustrate the expected phases of 2-5 nm.[1] The effects of the time interval of gas deletion and the molecular weight threshold for gas deletion on the end compositions were unclear. Also, the temperatures used were at highly elevated levels and might impact the thermodynamics.[27]

Starting from polymer precursor structure creation, this study quantitatively investigates how differing levels of carbon in the starting polymers and different polymer molecular structures affect the pyrolyzed ceramic compositions, yields, atomic structures, and bonds by using three polymer precursors: PDMS, polydiethylsiloxane (PDES), and SPR-684 polysiloxane (PSO). Such atomic evolution study during polymer to ceramic conversion provides new understanding about cluster formation and atomic separation. The simulated systems are also much larger, at ~100,000 atoms. In addition, a more realistic temperature range from 1500 K to 2100 K has been considered for pyrolysis.

2. Simulation framework

To initiate the simulations, PDMS, PDES, and PSO precursor structures were created first. Here, we use PSO as an example to explain the process. First, simulation codes were written using Python to create an idealized linear structure (Fig. 1a). The four side groups, -H, -CH_3, -C_2H_5, and -C_6H_5, were randomly distributed on the Si-O backbone. To achieve a random distribution that

would match the proportions of side groups in the actual commercial PSO SPR-684, which contains 59.3 wt% carbon (the high-carbon precursor in this study), each side group was weighted according to its abundance. This was done by randomly generating an integer from 1 to 7 and assigning 1-3 to the $-C_6H_5$ group, 4-5 to the $-C_2H_3$ group, 6 to $-C_2H_5$ group, and 7 to the -H group. The backbone of the initial structure consisted of 100 Si atoms and 100 O atoms.

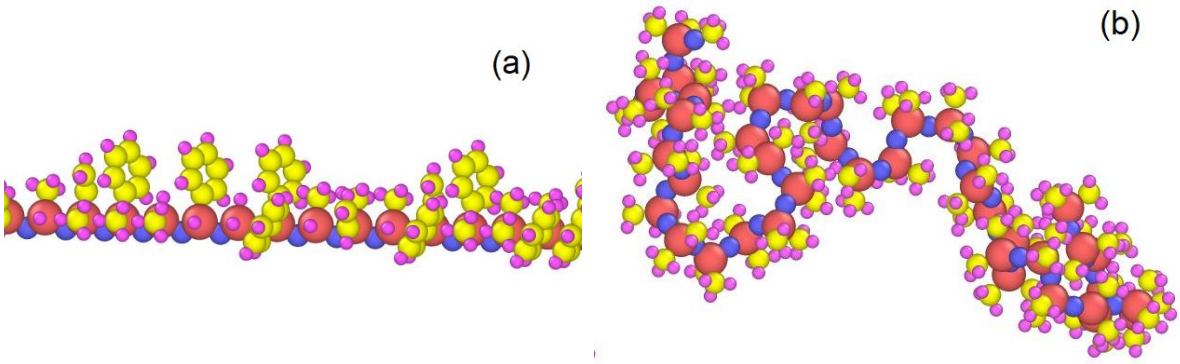

Fig. 1. a) Initial linear structure of PSO, b) a relaxed structure of PSO.

A ReaxFF energy potential[25, 28] in conjunction with LAMMPS [29] were used for the molecular dynamics simulation. The potential values used were generated specifically for polysiloxane to ceramic conversion systems.[25] The idealized structure in Fig. 1a still had significant strain as shown by the large increase in temperature when the simulation first started and was allowed to relax using NPT for 80,000 timesteps at 0.2 fs per timestep. The pressure in the system was set at 0 atm for complete structural relaxation. The potential energy of the system decreased significantly in the first 20,000 timesteps and then remained unchanged for the following 60,000 timesteps. The lack of change in the system energy indicated that the system had reached a fully relaxed state. Fig. 1b shows a 'relaxed' chain structure.

The "relaxed" chain was then duplicated 7 times to make 8 relaxed chains. These chains were randomly oriented with the center of each chain aligned to make a simple cubic stacking pattern (Fig. 2a). The 8 PSO chains were then allowed to undergo another "relaxation", allowing for the structure to consolidate and form a dense amorphous structure (Fig. 2b). The purpose of the relaxation step was to consolidate the distributed chains before the start of the pyrolysis. To simulate the relaxation process, the system was heated using NPT to 300 K under 2 atm and then allowed to run for 250,000 timesteps with each step being 0.2 fs.

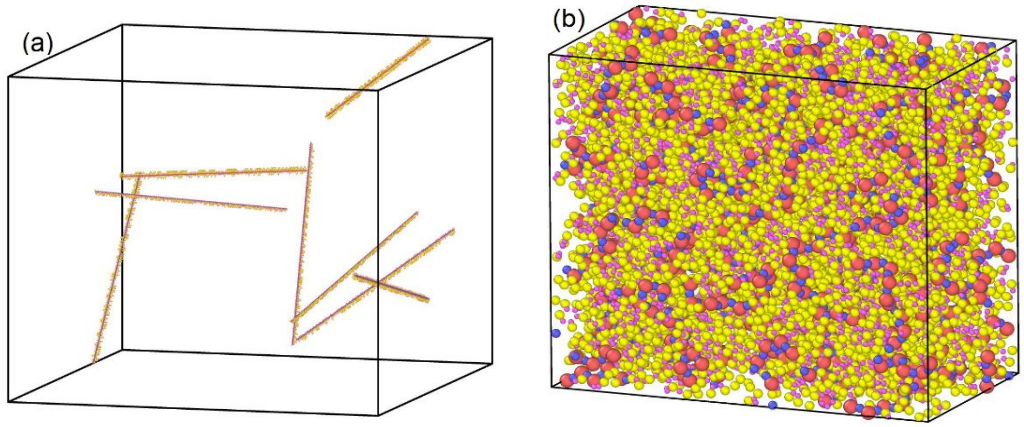

Fig. 2. a) Randomly distributed PSO chains after relaxation, b) consolidated PSO chains after homogenization.

The PSO system was further expanded to 93,680 atoms by duplicating the smaller and relaxed structure and then heated in an NPT system over the course of 0.5 ns from 300 K to 1500 K, 1800 K, and 2100 K in three parallel runs. The nature of the bonds was determined using the 'fix reax/c/bonds' command in LAMMPS, and a Python script was used to define the molecules based on the bonding data. During each of the heating phases the pressure was maintained at 2000 bar to prevent excessive system expansion. The timestep between the simulation runs was 0.2 fs. Gas species including CH_4, $H_3C\text{-}CH_3$, $H_2C{=}CH_2$, H_2, CO, CO_2, H_2O, O_2, CH_2O, and C_6H_6 were

periodically identified. Molecules matching the molecular weight of these species were then placed in a gas group in LAMMPS and deleted using an integrated Python script at 5 ps intervals.

Once the systems reached the peak temperatures, they were held at the temperatures for 2 ns. During this time the pressure remained constant at 2000 bar and the gas species were continuously deleted at the same 5 ps time intervals. After the holding phase, the system was gradually lowered in temperature back down to 300 K over the course of 0.5 ns for a total run time of 2.75-3 ns. Throughout the heating phase the bonding data were collected at 5 ps intervals and the atomic locations were tracked.

Two other polysiloxane systems of varying carbon contents were also created (Fig. S1). The systems consisted of PDMS containing 32.4 wt% carbon (low-carbon) and PDES containing 47.0 wt% carbon (mid-carbon). These systems were both created using the same procedure as for the PSO polymer above and were chosen based on their carbon contents. The low- and mid-carbon systems were also randomly distributed and allowed to consolidate. The PDMS system was expanded to 96,768 atoms and the PDES system contained 102,912 atoms. Both systems were heated in parallel to 1500 K, 1800 K, and 2100 K using the same process as for the PSO above. The systems were then held at the same 2 ns at the peak temperatures and allowed to cool using the same process. The gas species deleted were the same as those deleted in the PSO system and the interval of the gas deletion remained constant.

To extract RDF data from the simulation, the built-in LAMMPS function called ‘compute rdf’ was used. The RDF simulation was allowed to run at the peak temperature for each polymer system. The overall RDF results and the RDF results specific to all possible bonding groups were obtained. The RDF data extracted for all possible bonding groups were used to associate bonding with specific peak locations.

3. Results and discussion

3.1. Composition and yield

There is very little change in compositions for all three polymer systems after 1500 K pyrolysis as given in the supplement (Fig. S2). The main observations are slight Si and O composition increases and the H composition decrease for the PDES system. After 1800 K pyrolysis (Fig. S3), the Si and O compositions further increase and the H composition further decreases for the PDES system, which also leads to a slight C loss. The other two systems show the same trend but to a much less degree. For discussion purposes, the composition changes after 2100 K pyrolysis are given in Fig. 3. The compositions in the beginning 0.5 ns in Fig. 3 do not show significant changes because the systems undergo heating to reach the peak temperature.

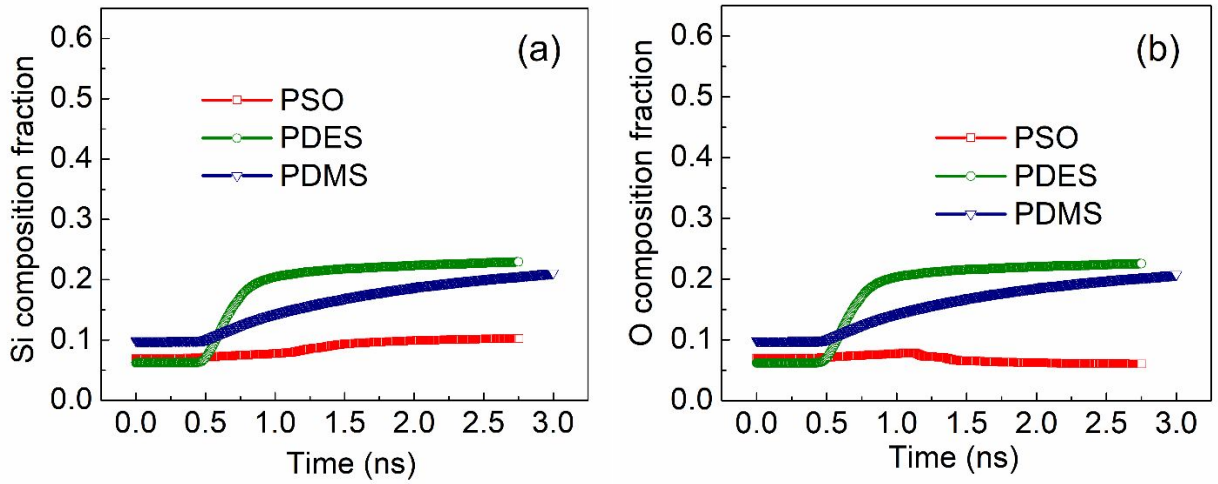

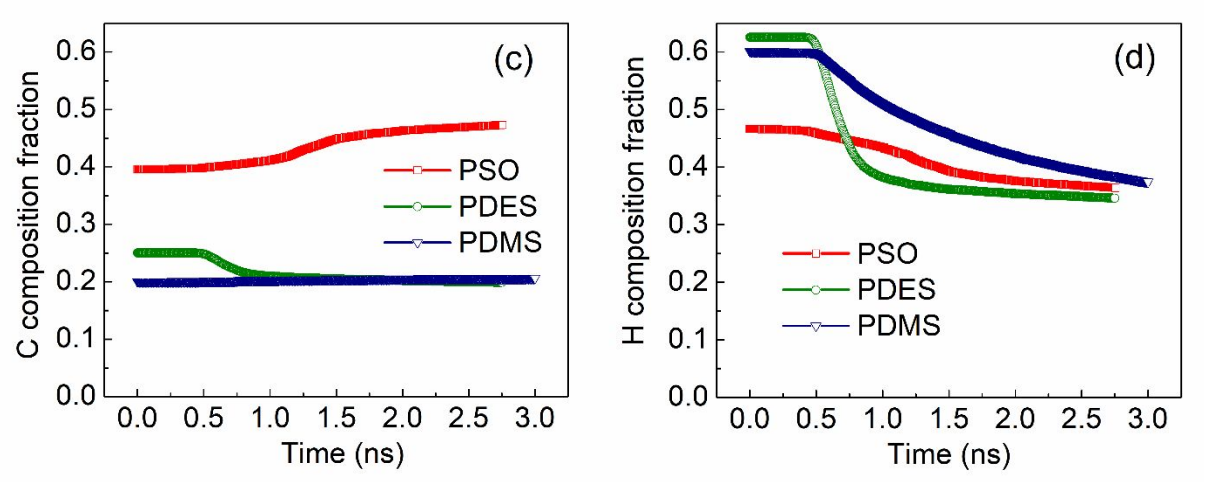

Fig. 3. Composition changes with time at 2100 K pyrolysis condition: a) Si, b) O, c) C, and d) H.

Fig. 3a shows the change of the Si content with the pyrolysis time as 2100 K. As with the low pyrolysis temperatures, the most significant change is from the PDES precursor, followed by the PDMS precursor and then by the PSO precursor. The Si atomic fraction starts at 0.10 and ends at 0.20 for the PDMS precursor and starts at 0.06 and ends at 0.23 for the PDES precursor. The PSO system has the smallest increase in the Si content at 2100 K, starting at 0.07 and ending at 0.10. The overall number of Si atoms is maintained consistent throughout the pyrolysis because Si is not a gaseous species to be deleted. The changes in the Si composition are due to the changes in the compositions of the other species through gas deletion.

Fig. 3b shows the O composition changes at 2100 K pyrolysis condition. The starting O atomic fraction for the PDMS system is 0.10 and increases gradually to 0.20. PDES follows a similar trend starting at 0.06 and increasing to a higher value of 0.23. The PSO precursor deviates compared to the other systems, starting at 0.07 and ending at 0.06. Examining Figs. 3a and 3b, PSO is the only system that does not have a 1:1 Si:O ratio during pyrolysis. The formation of C-O gaseous products accounts for the reduction in O in the PSO system.

The C content changes for each system at 2100 K are given in Fig. 3c. The PDMS precursor has little C composition change, starting at 0.20 atomic fraction and increasing slightly to 0.21 atomic fraction. The PDES system has a decrease from 0.25 to 0.20. The PSO system gains in the C content from 0.40 to 0.47. The decrease in the C content for the PDES system is related to the H loss as shown in Fig. 3d, likely through hydrocarbon species loss. The PSO system loses both H and O contents, leading to a relative increase in the overall C content. This is also related to the higher yield expected from the 6-C ring species (Fig. 4). These species more readily form graphitic groups and assist in reducing the H content while maintaining the C content.

The H content for each system at 2100 K can be seen in Fig. 3d. The PDMS system shows a large decrease in the H content from 0.60 to 0.37, which is mirrored by the increase in relative O and Si contents from 0.10 to ~0.20. The PDES system has an even larger drop in the H content from 0.63 to 0.35. It also has the largest Si and O content increases from 0.06 to 0.23. The PSO behaves similarly with a loss of 0.11 (from 0.47 to 0.36) in H. The highest level of H loss is present in the polymer with the largest linear side group, PDES. The higher hydrocarbon content of the PDES precursor leads to more available C to form gas(es). The methyl side group in the PDMS system leads to the second largest decrease in the H content.

In earlier experimental studies, PSO pyrolyzed at 1300°C had a yield of ~76%.[2, 15] At 1500°C condition, the yield further decreased to 72.5%. Fig. 4 shows that the PDMS system has the intermediate yield of 99.1%, 92.3%, and 78.0% at 1500 K, 1800 K, and 2100 K pyrolysis temperatures. Again, there are no significant changes in the beginning 0.5 ns because the systems undergo heating to reach the peak temperature. The yield data show the most significant mass loss in the PDES system. The end yields are 88.7%, 60.8%, and 54.5% for the respective temperatures of 1500 K, 1800 K, and 2100 K. The PSO has a yield of 97.7%, 96.4%, and 80.8% respectively.

Such results mean that 1500 K is too low a pyrolysis temperature for the polymer to ceramic conversion; the simulation temperature is not directly comparable with the experimental temperature. Also, the amount of simulation time at each peak temperature is much shorter (ns vs. hrs) due to computation speed limitation. Because of this, the simulation results are more akin to pyrolysis through fast heating using a laser source, a very short duration of heating.

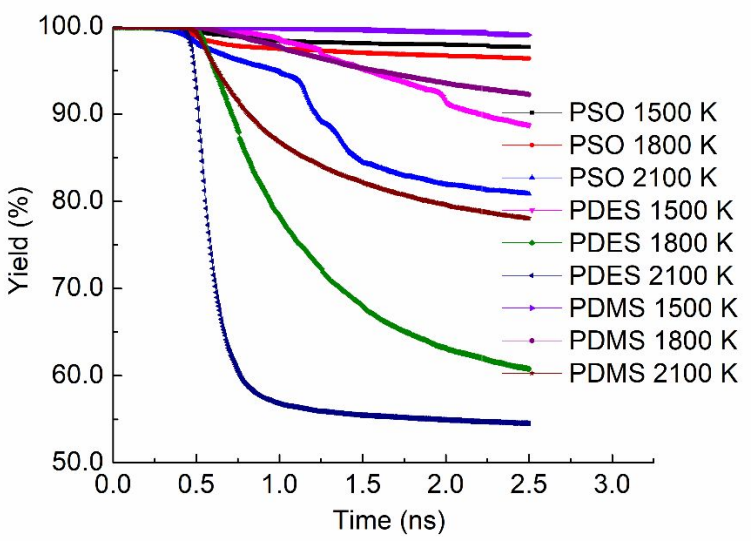

Fig. 4. Yield results for the three polymer systems after simulation at three pyrolysis temperatures.

The difference in yield shows that the carbon amount and the side group atomic structure in the precursors have a large impact. In the PSO system, the carbon species have more 6-C ring members and higher yields. PDES has intermediate carbon species such as ethyl groups, yet the yield is lowest. On the other hand, PDMS has even smaller methyl side groups while the ceramic yield is at an intermediate level. Thus, it can be stated that the pyrolytic fragmentation and the ceramic yield are related to the polymer precursor molecular structure.[30, 31] The cleavage of the polymer side group is related to its bonding strength with the polymer backbone, e.g., the methyl group seems to bond stronger than the ethyl group, which leads to a higher ceramic yield,

especially at lower pyrolysis temperatures. More 6-C ring side groups also lead to a higher yield. At higher pyrolysis temperatures, the cleavage of the Si-O linear backbone may become significant.[30]

3.2. Atomistic structure evolution

Fig. 5 shows the starting PDMS structure and the structures at each simulation temperature (1500 K, 1800 K, and 2100 K) after 2.0 ns holding time. The starting structure (Fig. 5a) has no distinguishable regions forming. It is homogeneous at the atomistic scale. The 1500 K structure (Fig. 5b) has some rather small Si-O fractals; the overall atomic structure is still uniform. Fig. 5c shows that the SiOC clusters grow to 0.5-2 nm size after 1800 K pyrolysis. The SiOC clusters are randomly distributed; there is minimal clustering of C. Fig. 5d shows that after 2100 K pyrolysis the SiOC amorphous regions become more connected; there is a continuous network spanning over the entire simulation cell; both Si-O rich and C-rich regions co-exist. Because of the intrinsic thermodynamic stability of Si-O clusters and C domain themselves, Si-O and C tend to separate. The cluster separation boundaries are diffused. There is still significant C mixing within the Si-O clusters and O mixing in the C-rich clusters. H atoms only co-exist with C species.

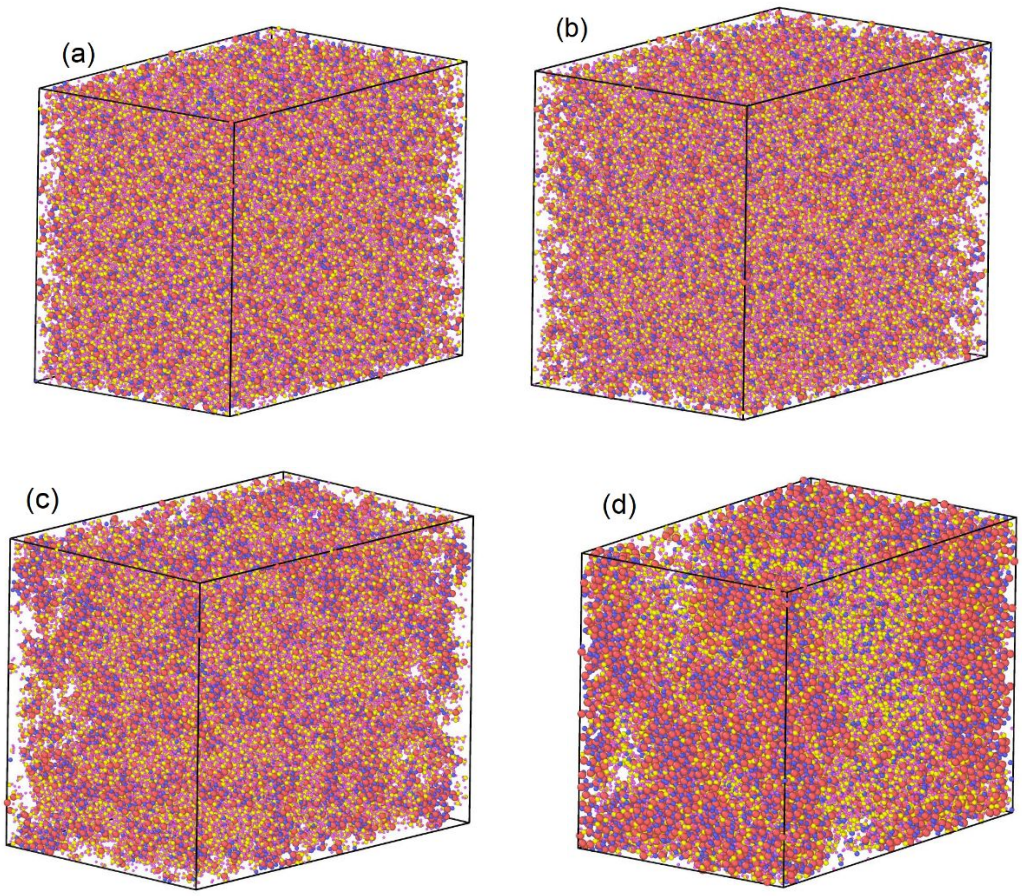

Fig. 5. Atomic structural evolution for PDMS: a) starting PDMS structure, b) 1500 K, c) 1800 K, and d) 2100 K. In all the images, the color scheme is as follows: Si-red, O-blue, C-yellow, and H-pink.

Fig. 6 shows the atomistic structures of the PDES precursor system at different states of pyrolysis. Fig. 6a is the starting structure, demonstrating a homogeneous atomic distribution with short Si-O strings. There is a higher C content. After pyrolysis at 1500 K (Fig. 6b), the structure remains homogenous, the same as for the PDMS system (Fig. 5b). However, the SiOC clusters are larger, at 1-2 nm, throughout the system. It also shows more Si-O and C cluster separation. A more dramatic structural change can be seen in Fig. 6c for the 1800 K pyrolysis condition. There is

significant segregation of Si-O and C regions. For the 2100 K pyrolysis condition (Fig. 6d), the Si-O and C clusters form completely separated regions, with almost no C presence in the Si-O region and almost no Si-O presence in the C-rich region. H continues to co-exist with the C species.

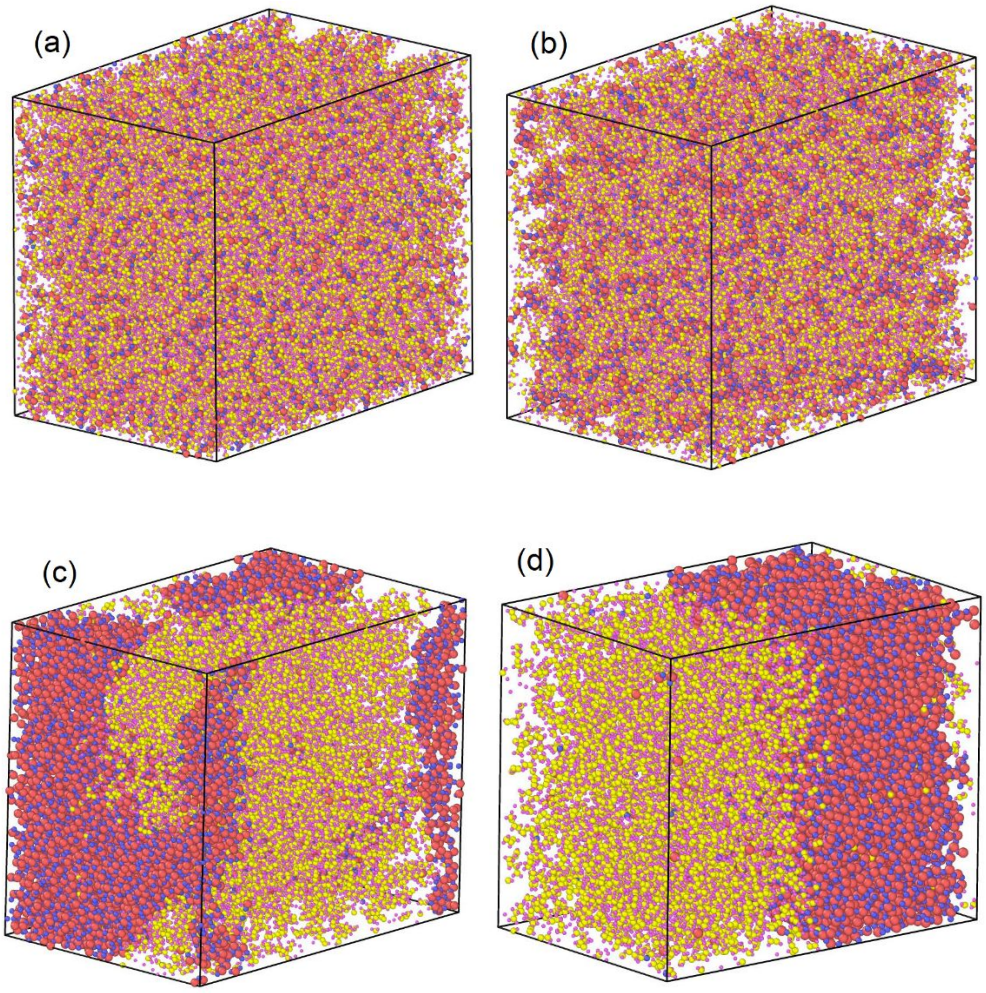

Fig. 6. Atomic structural evolution for PDES: a) starting PDES structure, 2) 1500 K, b) 1800 K, and c) 2100 K. In all the images, the color scheme is as follows: Si-red, O-blue, C-yellow, and H-pink.

Fig. 7 shows the same atomic structure series for the PSO system. At the start of the pyrolysis, the PSO system already has an atomic structure with Si-O fractals and more separated

C-rich regions, as shown in Fig. 7a. The other significant difference is that many 6-C rings appear, due to the C-rich nature of the PSO precursor, indicating planer C formation. After 1500 K pyrolysis, Si-O rich and C-rich regions continue to grow and separate (Fig. 7b). After pyrolysis at 1800 K, as seen in Fig. 7c, there are notable Si-O regions ranging in size from 1 nm to 5 nm. The phase separation degree is in-between those of the PDMS and PDES systems. The C-rich regions continue to evolve with many 6-C rings and form networks with a higher level of C-C bonding. There are distinguishable C regions at this stage. Fig. 7d shows the most significant change in the atomic structure. Most of the Si-O species can be observed in a single large particle with some Si-O clusters in smaller regions interspersed in the C matrix. 6-C rings evolve into string and connected structures, a precursor for turbostratic C. Even though PSO has the most C content among the three polymer systems, the Si-O cluster and C-rich region separation is not as extensive as for the PDES system after 2100 K pyrolysis. H continues to co-exist with C species. This again indicates that atomic structural evolution is a function of both the composition and the molecular structure of the polymer precursors.

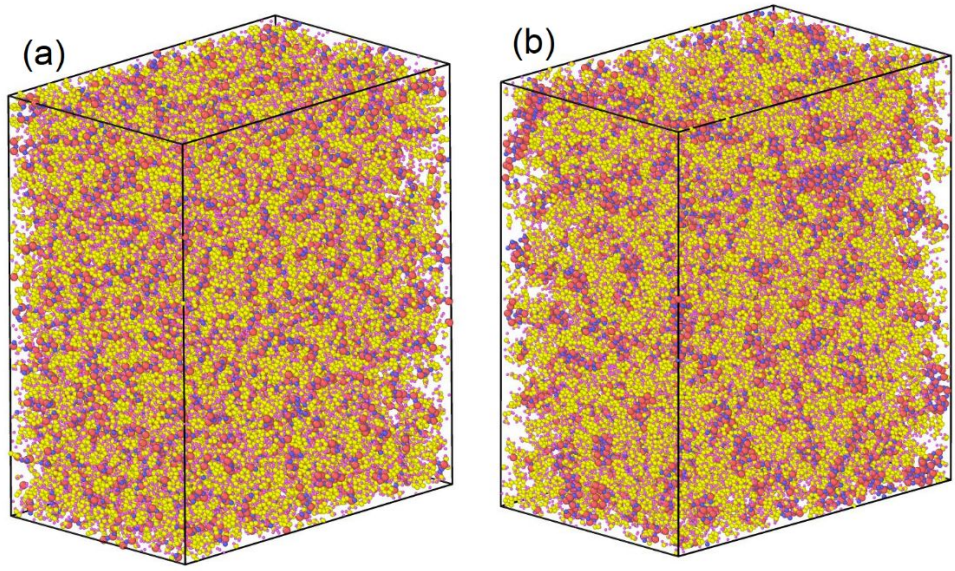

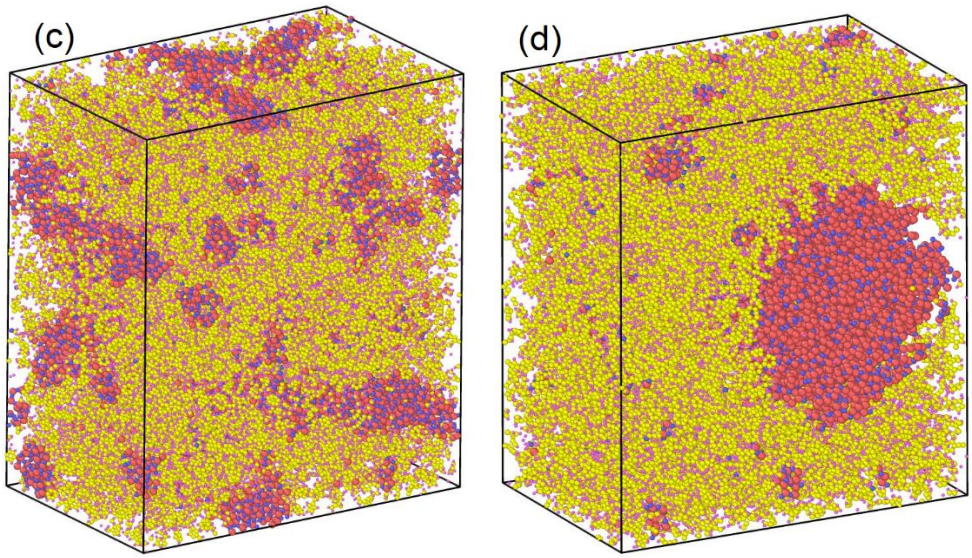

Fig. 7. Atomic structural evolution for PSO: a) starting PSO structure, 2) 1500 K, b) 1800 K, and c) 2100 K. In all the images, the color scheme is as follows: Si-red, O-blue, C-yellow, and H-pink.

The presence of H species, though has been reported by other studies,[10, 24] has not been shown to preferentially co-exist with the C-rich regions. The intermixing tendency of the Si-O rich region and the C-rich region is also uniquely illustrated in this work. Both are related to polymer molecular structures. In the polymer, C-H bond results in the H co-existence with C. The mixed side groups (-C_6H_5 group, -C_2H_3 group, -C_2H_5 group, -H group) in PSO likely lead to less cluster separation than PDES.

3.3. Bond changes

Bond data were extracted for each system as shown in Fig. 8 for the 2100 K pyrolysis condition. The 1500 K and 1800 K data show similar trends, and the results can be found in the

supplement (Figs. S4 and S5). In general, a lower pyrolysis temperature induces less bond changes in comparison to a higher pyrolysis temperature.

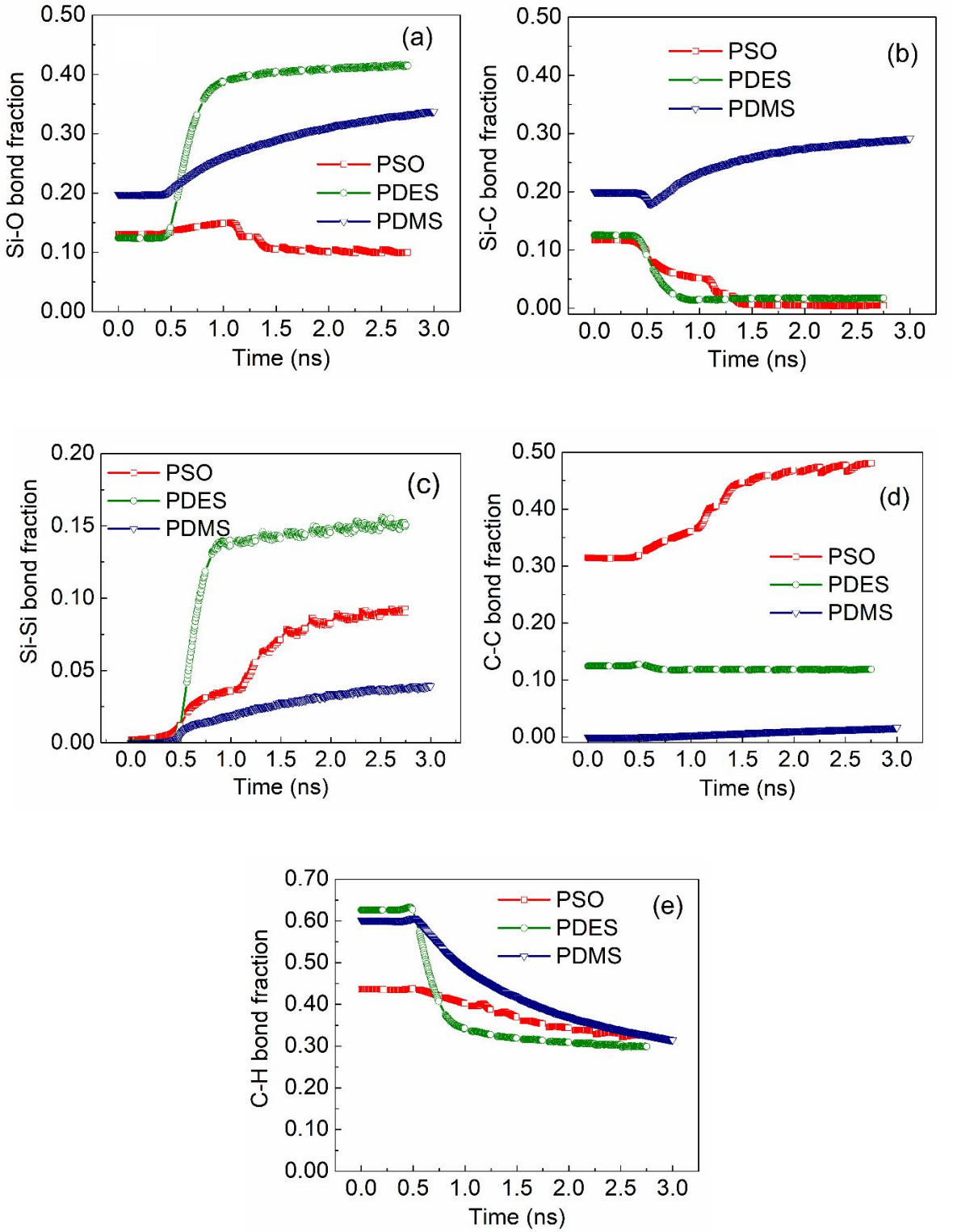

Fig. 8. Bond fractions of different polymer precursor systems after 2100 K pyrolysis simulation: a) Si-O bond, b) Si-C bond, c) Si-Si bond, d) C-C bond, and e) C-H bond.

Fig. 8a shows the Si-O bond change with the simulation time for the 2100 K pyrolysis condition. For the PDMS precursor, there is a 0.14 atomic fraction increase in the Si-O bond fraction. This is correlated with the Si-C bond increase (Fig. 8b) and the lower level of Si-Si bond formation (Fig. 8c). Such changes indicate that PDMS has no fundamental C side group cleavage from the backbone. As seen later in Fig. 8e, the changes are mainly due to the C-H bond loss. In the PDES system, the Si-O bond fraction increases by 0.29 at 2100 K temperature (Fig. 8a). Fig. 8b shows that the PDES has Si-C bond fraction loss, which correlates with the Si-O bond and Si-Si bond fraction increases (Figs. 8a and 8c). This collectively means the PDES polymer side group decomposition and new Si-rich cluster formation. While the Si-Si bonding is less favorable, Si-Si bonds may be formed to reduce the dangling Si bonds once the Si-C bonds are broken and the C clusters become separated. For the PSO system, the Si-O bond fraction decreases by 0.03 at 2100 K. The loss in Si-O bonds correlates with the loss in Si-C bonds (Fig. 8b) and the increase in Si-Si bonds (Fig. 8c). This means that the C side group and the Si-O backbone are broken during pyrolysis, the highly active Si-O radicals form Si-Si bonds. As a result, Fig. 8(c) shows increases in the Si-Si bonds for all the three polymer systems, indicating that the Si-Si bonding/close coordination becomes more significant. The larger increase in the Si-Si bond fraction in the PDES system (Fig. 8c) than in any other system is related to the significant Si-C bond loss (Fig. 8b) and the largest C-H bond loss (Fig. 8e).

The C-C bond fraction increases from PDMS, to PDES, and to PSO, consistent with the atomic structures shown in Figs. 5d, 6d, and 7d. All the polymer systems show a decrease in C-H

bonds (Fig. 8e) at 2100 K, at 0.29, 0.33, and 0.11 for PDMS, PDES, and PSO respectively. This means that the C-H bond change is sensitive to the type of hydrocarbon groups. PSO forms more C-C bonds while the C-H bond loss is the least.

Both PDES and PSO demonstrate Si-C bond decrease to zero at 2100 K as shown in Fig. 8b. The cleavage of Si-C bonds is more apparent in larger C-containing groups, suggesting that under high temperatures the larger C groups impose more stress on the Si-C bonds, which leads to more Si-C cleavage. PDMS instead has a 0.09 Si-C bond fraction increase. As stated, the increase is due to the loss of C-H bonds as shown in Fig. 8e. PDMS has a mass loss comparable to that of PSO (Fig. 4). Even though the methyl groups on the Si-O backbone of PDMS have a weaker proclivity to form C networks (negligible C-C bonds in Fig. 8d); smaller C side groups are more effective in maintaining the Si-C bonds and thus resulting in a lower mass loss during pyrolysis. PDES and PSO, however, lose most of their C side groups at 2100 K pyrolysis temperature with different C-C bond formation. This shows that the type of C-containing side group in the polymer precursors plays a major role in the formation of Si-O and C regions.

3.4. Radial distribution function

The RDF data for the PDES system at different pyrolysis temperatures are given in Fig. 9a. The corresponding data for the other systems can be found in the supplement (Fig. S6) and Fig. 9b. The latter shows the 2100 K pyrolysis results for all three polymer systems. In both Figs. 9a and 9b, the highest peak corresponds to the C-H peak. This is due to the limited simulation time, not allowing for complete H removal. In the PDES system (Fig. 9a), the C-H peak decreases with the pyrolysis temperature increase as more H is removed. In addition, at 1.36 Å distance, a C-C peak is not observed for the 1500 K pyrolysis condition but is present for the 1800 K pyrolysis

condition and becomes stronger at 2100 K. This means that a higher pyrolysis temperature leads to more C-C bonds. The second largest peak at 1.59 Å is the Si-O peak. At all the pyrolysis temperatures, PDES retains a significant amount of Si-O bonds. A higher pyrolysis temperature leads to more Si-O bonds. However, beyond this bond length, other bond peaks are negligible, with a minor Si-C bond for the 1500 K condition. This minor Si-C bond peak at 1500 K is from the original Si-C bonds in the polymer, which disappears for the higher temperature conditions. There are even smaller amounts of Si-Si and outer shell C-C bonds. It should be noted that the Si-Si/C-C bond peak becomes weaker with the pyrolysis temperature increase, consistent with its transient nature. The extremely variable nature of the Si-Si distribution gives very broad peaks compared to other bonds. For all the pyrolysis temperatures, there are no significant peaks at distances beyond 2.5 Å, indicating that the systems are highly amorphous.

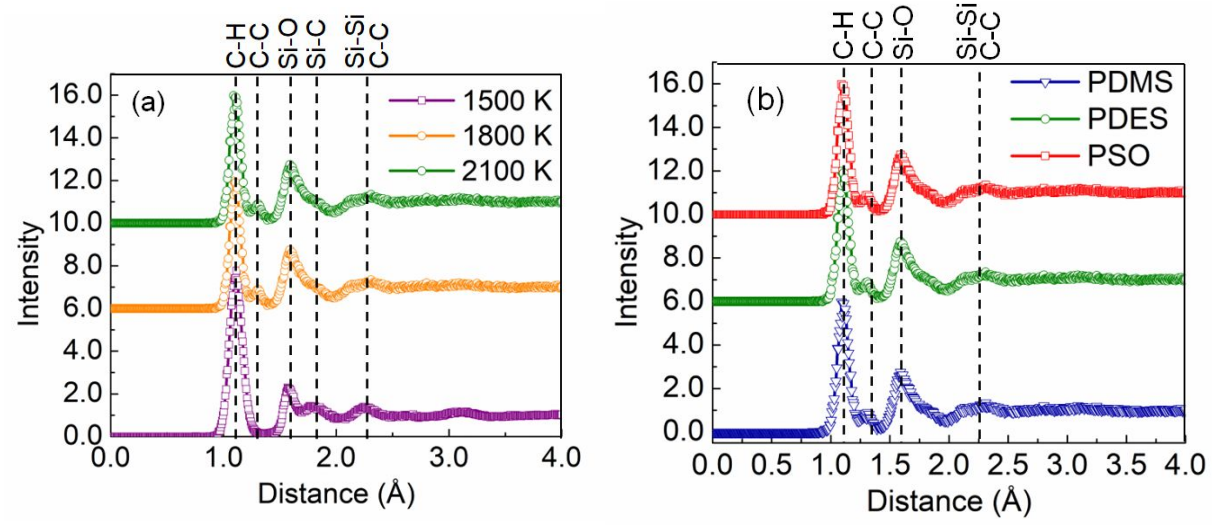

Fig. 9. RDF results of different polymer systems: a) PDES at different pyrolysis temperatures, b) all three precursors after 2100 K pyrolysis.

After 2100 K pyrolysis (Fig. 9b), the C-H peak continues to be present for each system because H is hard to be removed. Regardless, all three systems have the C-C peak, indicating C cluster formation even though the specific cluster size is not directly represented in Fig. 9b. The Si-O and Si-Si/C-C bonds continue to be present. However, the Si-Si/C-C peak is weak, meaning its low amount. Again, for all the precursor conditions after 2100 K pyrolysis, there are no significant peaks at distances beyond 2.5 Å. The systems have no long-range ordering.

4. Conclusions

This study is focused on advancing the ReaxFF simulation of polymer derived SiOC ceramics and understanding the effects of polymer precursors with different carbon content on the composition, atomic structure evolution, bonding, and RDF of the resulting ceramics at a quantitative level. A higher level of carbon in the polymer leads to greater separation between Si-O rich and C-rich regions. Cyclical C side groups results in a higher yield, followed by the polymer with smaller C-containing side groups. The polymer with smaller C-containing side groups maintains higher levels of Si-C bonding and the polymer with larger C-containing side groups results in higher degrees of C-rich regions. A higher C precursor leads to more C-C bonds and less Si-O bonds. This work provides important insights into the atomic structural evolution of different polymer systems during pyrolysis.

Acknowledgment

The authors would like to acknowledge the financial support from the National Science Foundation under Grant No. CBET-2024546 and Air Force Office of Scientific Research under grant number FA9550-22-1-0081.

Data availability:

The data required to reproduce these findings are available to download from https://data.lib.vt.edu.

Supporting information:

Molecular structures of PDMS and PDES, composition changes after 1500 K and 1800 K pyrolysis simulations, bond fraction data after 1500 K and 1800 K pyrolysis simulations, and RDF data after 1500 K and 1800 K pyrolysis simulations.

References:

1. Wen, Q.; Yu, Z.; Riedel, R., The fate and role of in situ formed carbon in polymer-derived ceramics. *Progress in Materials Science* **2020,** *109*, 100623.
2. Rau, A. V.; Knott, K.; Lu, K., Porous SiOC/SiC ceramics via an active-filler-catalyzed polymer-derived method. *Materials Chemistry Frontiers* **2021,** *5* (17), 6530-6545.
3. Greil, P., Polymer derived engineering ceramics. *Advanced Engineering Materials* **2000,** *2* (6), 339-348.
4. Lu, K.; Erb, D., Polymer derived silicon oxycarbide-based coatings. *International Materials Reviews* **2018,** *63* (3), 139-161.
5. Duan, W. Y.; Yin, X. W.; Li, Q.; Schlier, L.; Greil, P.; Travitzky, N., A review of absorption properties in silicon-based polymer derived ceramics. *Journal of European Ceramic Society* **2016,** *36* (15), 3681-3689.

6. Lu, K.; Erb, D.; Liu, M. Y., Thermal stability and electrical conductivity of carbon-enriched silicon oxycarbide. *Journal of Materials Chemistry C* **2016,** *4* (9), 1829-1837.
7. Brequel, H.; Parmentier, J.; Sorar, G. D.; Schiffini, L.; Enzo, S., Study of the phase separation in amorphous silicon oxycarbide glasses under heat treatment. *Nanostructured Materials* **1999,** *11* (6), 721-731.
8. Grassie, N.; Macfarlane, I. G., The thermal degradation of polysiloxanes—I. Poly(dimethylsiloxane). *European Polymer Journal* **1978,** *14* (11), 875-884.
9. Grassie, N.; Macfarlane, I. G.; Francey, K. F., The thermal degradation of polysiloxanes—II. Poly(methylphenylsiloxane). *European Polymer Journal* **1979,** *15* (5), 415-422.
10. Gao, H. F.; Wang, H. J.; Zhao, Z. H.; Niu, M.; Su, L.; Wei, Y., Reactive dynamics simulation study on the pyrolysis of polymer precursors to generate amorphous silicon oxycarbide structures. *Journal of Physical Chemistry C* **2018,** *122* (10), 5767-5773.
11. Wang, X.; Wu, J.; Li, Y.; Zhou, C.; Xu, C., Pyrolysis kinetics and pathway of polysiloxane conversion to an amorphous SiOC ceramic. *Journal of Thermal Analysis and Calorimetry* **2014,** *115* (1), 55-62.
12. Saha, A.; Raj, R., Crystallization maps for SiCO amorphous ceramics. *Journal of the American Ceramic Society* **2007,** *90* (2), 578-583.
13. Bawane, K.; Erb, D.; Lu, K., Carbon content and pyrolysis atmosphere effects on phase development in SiOC systems. *Journal of the European Ceramic Society* **2019,** *39* (9), 2846-2854.
14. Erb, D.; Lu, K., Synthesis of SiOC using solvent-modified polymer precursors. *Materials Chemistry and Physics* **2019,** *237*, 121844.

15. Ma, R.; Lu, K.; Erb, D., Effect of solvent in preparation of SiOC bulk ceramics. *Materials Chemistry and Physics* **2018,** *218*, 140-146.

16. Wang, L.; Lu, K.; Ma, R., Effects of different polymer precursors on the characteristics of SiOC bulk ceramics. *Applied Physics A* **2019,** *125* (6), 395.

17. Erb, D.; Lu, K., Effect of additive structure and size on SiO_2 formation in polymer-derived SiOC ceramics. *Journal of the American Ceramic Society* **2018,** *101* (12), 5378-5388.

18. Kroll, P., Modelling polymer-derived ceramics. *Journal of the European Ceramic Society* **2005,** *25* (2-3), 163-174.

19. Kroll, P., Modelling and simulation of amorphous silicon oxycarbide. *Journal of Materials Chemistry* **2003,** *13* (7), 1657.

20. Kroll, P., Searching insight into the atomistic structure of SiCO ceramics. *Journal of Materials Chemistry* **2010,** *20* (46), 10528-10534.

21. Bai, W. R.; Widgeon, S.; Sen, S., Structure and topological characteristics of amorphous silicon oxycarbide networks: Results from Reverse Monte Carlo simulations. *Journal of Non-Crystalline Solids* **2014,** *386*, 29-33.

22. Szczypka, W.; Kolezynski, A., Molecular mechanics modelling of amorphous silicon oxycarbide clusters by bottom-up approach. *Journal of Molecular Structure* **2020,** *1208*, 127930.

23. Chenoweth, K.; Cheung, S.; Van Duin, A. C. T.; Goddard, W. A.; Kober, E. M., Simulations on the thermal decomposition of a poly(dimethylsiloxane) polymer using the ReaxFF Reactive Force Field. *Journal of the American Chemical Society* **2005,** *127* (19), 7192-7202.

24. Naserifar, S.; Liu, L.; Goddard, W. A.; Tsotsis, T. T.; Sahimi, M., Toward a process-based molecular model of SiC membranes. 1. Development of a Reactive Force Field. *The Journal of Physical Chemistry C* **2013,** *117* (7), 3308-3319.
25. Ponomarev, I.; van Duin, A. C. T.; Kroll, P., Reactive Force Field for simulations of the pyrolysis of polysiloxanes into silicon oxycarbide ceramics. *The Journal of Physical Chemistry C* **2019,** *123* (27), 16804-16812.
26. Sorarù, G. D.; Pederiva, L.; Latournerie, J.; Raj, R., Pyrolysis kinetics for the conversion of a polymer into an amorphous silicon oxycarbide ceramic. *Journal of the American Ceramic Society* **2002,** *85* (9), 2181-2187.
27. Weimer, A. W.; Nilsen, K. J.; Cochran, G. A.; Roach, R. P., Kinetics of carbothermal reduction synthesis of beta silicon carbide. *AIChE Journal* **1993,** *39* (3), 493-503.
28. van Duin, A. C. T.; Dasgupta, S.; Lorant, F.; Goddard, W. A., ReaxFF: A Reactive Force Field for hydrocarbons. *The Journal of Physical Chemistry A* **2001,** *105* (41), 9396-9409.
29. Aktulga, H. M.; Fogarty, J. C.; Pandit, S. A.; Grama, A. Y., Parallel reactive molecular dynamics: Numerical methods and algorithmic techniques. *Parallel Computing* **2012,** *38* (4-5), 245-259.
30. Hurwitz, F. I.; Kacik, T. A.; Bu, X. Y.; Masnovi, J.; Heimann, P. J.; Beyene, K., Pyrolytic conversion of methylsilane and vinylsilane polymers to Si-C ceramics. *Journal of Materials Science* **1995,** *30* (12), 3130-3136.
31. Shieh, Y. T.; Sawan, S. P., Hydropolysilanes as precursors to silicon-carbide. *Journal of Applied Polymer Science* **1995,** *58* (11), 2013-2024.

TOC Graphic

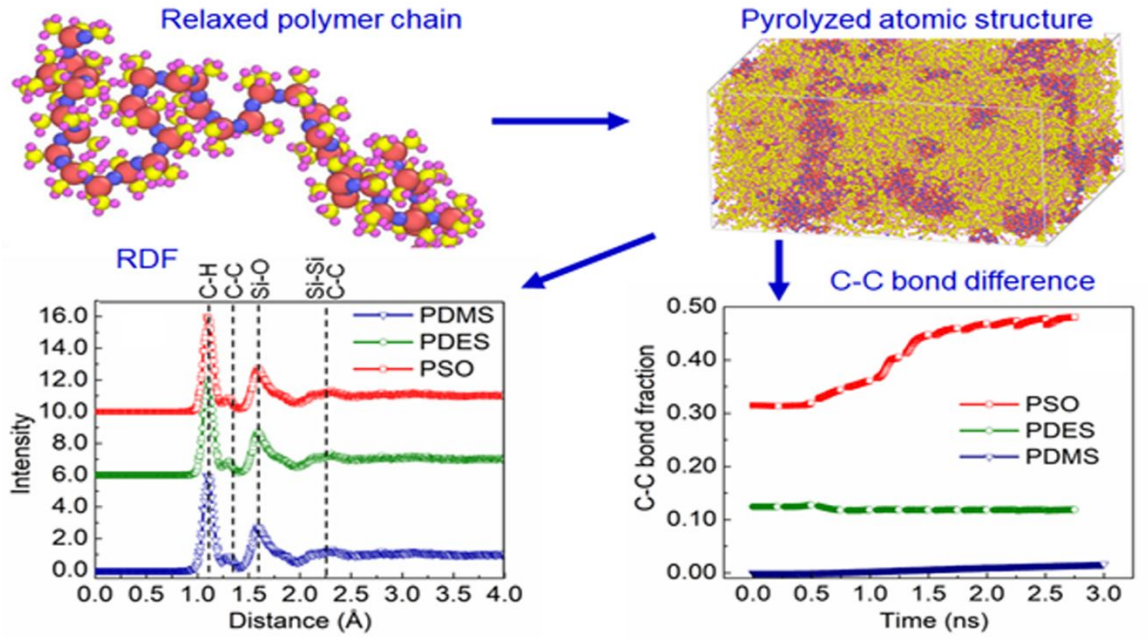
Relaxed polymer chain
Pyrolyzed atomic structure
RDF
C-H
C-C
Si-O
Si-Si
C-C
PDMS
PDES
PSO
Intensity
Distance (Å)
C-C bond difference
C-C bond fraction
Time (ns)